Surface Transfer Impedance Characterization of Shielded Cables

Rodrigo Cabaleiro Cortizo Freire
Chief Engineer Office
EMBRAER
São José dos Campos - SP, Brasil.
rodrigo.freire@embraer.com.br

José Antônio de Souza Mariano
Chief Engineer Office – EMBRAER
ITA – Instituto Tecnológico de Aeronáutica
São José dos Campos - SP, Brasil.
jose.mariano@embraer.com.br

***Abstract*— Advances in the electronic industry have allowed a greater number of electronic equipment performing critical functions onboard civil aircraft. Therefore, immunity against lightning induced transients and High Intense Radiated Fields (HIRF) has become a significant issue to manage in the early stages of product development. The surface transfer impedance is an intrinsic parameter that represents the effectiveness of the cable shielding and is a key parameter for understanding electromagnetic compatibility (EMC) problems as well as an important input parameter to computational electromagnetic models (CEM). Such models are useful to predict voltages and currents at equipment interfaces during a lightning event for example. In this study transfer impedance measurements of a coaxial cable, a single shielded wire and a twisted shielded pair have been carried out according to the line injection and triaxial test methods standardized by the International Electro technical Commission (IEC). To validate the approach, experimental results have been compared to the analytical estimates.**

Keywords*— *CEM; EMC; shielded cables; surface transfer impedance.

I. INTRODUCTION

Technological advances in the area of electronic systems have allowed a greater number of electronic based-systems to perform critical functions in the maintenance of airworthiness e.g. engine control, navigation, instrumentation and flight control systems [1],[2].

In the resultant electromagnetic environment, the ability of embedded systems to operate in compatibility becomes a challenge [3]. Beyond the others aircraft equipment that may be a source of interference, the systems must be designed and installed to provide effective protection against the external sources of potential interference such as HIRF and the indirect effects associated with lightning strikes.

One possible way to manage coupling into the electronic interfaces is to protect the harnesses by adding layers of shielding. On the other hand, the amount of additional weight on signal cables must be optimized to avoid the unnecessary payload that is ultimately translated into operational cost.

To evaluate how much protection will provide the required attenuation it is important to map the possible coupling paths, characterize the shielding properties of each relevant feature and estimate the signals induced on equipment interfaces due to design variations by computer simulations.

The surface transfer impedance is an intrinsic parameter that represents the shielding effectiveness as a function of geometrical features and electrical properties of shielding materials [4]. It is a key parameter in the determination of the electromagnetic coupling into electronic circuitry or radiated emissions from signals flowing through their harnesses.

This paper presents a practical and analytical investigation of the surface transfer impedance of typical cables used in aircraft systems. The experimental characterization of the transfer impedance was conducted according to the line injection and triaxial test methods suggested in the IEC 62153. The test results have also been compared to the analytical estimates from the formulations proposed by Vance [5], Kley [6] as well as to full wave time domain simulations with the transmission line matrix (TLM) method.

II. DEFINITION OF SURFACE TRANSFER IMPEDANCE

Surface transfer impedance, initially introduced by Schelkunoff in [7], is defined as the ratio between induced voltage in the shield inner surface and the current flowing on shield external surface per unit length as in (1).

$$Z_t = \frac{dV}{dz}\frac{1}{I_0} \quad (1)$$

Where,

dV/dz is the rate of change in voltage on the inner surface of shield per unit length [V/m];

I_0 is the current flowing through the shield on its outer surface [Amps];

Z_t is the cable shield surface transfer impedance per unit lenght [Ω/m].

III. MEASUREMENT METHODS

The two measurement methods proposed by IEC 62153 in [8] and [9] were applied in this paper to characterize the

transfer impedance of cables with different shielding constructions.

A. *Triaxial Method*

The triaxial method has this nomenclature due to the existence of three coaxial cylinders: an outer tube concentric to the cable, the shield under test and the inner conductor. The tube encloses the shield so that it becomes the main conductor of a coaxial transmission line and conducts a known current provided by a signal generator or a network analyzer [10]. The induced voltage at the central conductor, due to this current flowing on its shield, is measured with a receiver or a network analyzer.

This system can be analyzed as two transmission lines, with line 1 being composed by the outer cylinder and the shielding of the cable, and line 2 formed by the inner conductor of the cable under test with its shield. These lines are coupled by the transfer impedance of the shield [10].

B. *Line Injection Method*

It is a simpler configuration for transfer impedance measurement since it does not require a cylinder concentric to the cable. The method consists in injecting a known signal into a metal strip positioned on top of the cable to be tested so as to produce an electromagnetic radiation in the vicinity of the cable, causing a current to flow in its shield. Due to shield transfer impedance, a voltage will be induced in the cable core. This voltage is then measured with a network analyzer connected at one end while the other is terminated with matched impedance.

The metal strip has its width, W, designed so that the transmission line formed with the shield has a characteristic impedance of 50 Ω, in order to obtain an impedance match with the output circuit of the generator. Equation (2) expresses the necessary relationship between the plate width and its distance from the cable shield to obtain the desired characteristic impedance [11].

$$\frac{W}{H} = \left(\frac{377}{\sqrt{\varepsilon_r} Z_0} - 2\right) \tag{2}$$

Where,

W is the width of the strip [mm];

H is the distance between the strip and the cable screen [mm];

ε_r is the relative electrical permittivity of the dielectric of the coating;

Z_0 is the desired characteristic impedance for the line [Ω];

In the line injection method the shield is not short circuited at one end, in this way, both the transfer impedance and the capacitive coupling act on the cable at the same time. Therefore, the result obtained is the sum of the transfer impedance and the capacitive coupling impedance, resulting in the equivalent transfer impedance, Z_{te}. However, for shields with good optical coverage this capacitive coupling is practically insignificant [8].

IEC 62153 Part 4-3 and Part 4-6 presents the setups for transfer impedance measurement, providing for each case the expression for the Z_t calculation in function of the scattering parameter S_{12} measured with the network analyzer. For triaxial setup used in this paper the measurement cut-off frequency is 30 MHz per meter, whereas for line injection method the cut-off frequency depends on dielectric material permittivity of cable jacket and injection circuit insulating.

IV. Simulation Model

The three-dimensional electromagnetic simulation of a coaxial cable was performed using the Microwave Studio module of commercial software CST – Computer Simulation Technology Studio Suite [12].

Due to the very small diameters of the shield filaments a detailed model would lead to a greater refinement in mesh, resulting in a large number of cells and therefore a long simulation time. In this way, a simplified model was proposed so that the simulation time is feasible. In addition, the time domain analysis was chosen because the Transmission Line Matrix (TLM) algorithm allows to modeling the shielding thickness internally, not requiring it to be considered in the mesh refinement.

In order to reduce the computational volume the simulated cable was a RG58 with 10 mm length. Since Z_t is given in ohms per meter the value obtained can be extrapolated to the real length in a post processing task. The inner conductor was modeled as a copper cylinder whose electrical conductivity is 5.8×10^7 S/m. The dielectric surrounding this conductor was a polyethylene with relative permeability of ε_R = 2.25. The dimensions of this cable are illustrated in Fig. 1. The shield, consisting of 36 AWG tinned copper filaments, was modeled as a thin panel of thickness d equal to 0.127mm and an electrical conductivity of 5.4×10^7 S/m. Shield apertures, shown in Fig. 2, were modeled according to the Vance definition.

A. *Line Injection Method Simulation*

Similarly to the measurement procedure with a vector network analyzer, a discrete S-parameter port was added between the shield and the injection line, while another was added between the central wire conductor and the shield. At the opposite ends two 50Ω loads were inserted to proper matching with the characteristic impedance of the inner and outer lines.

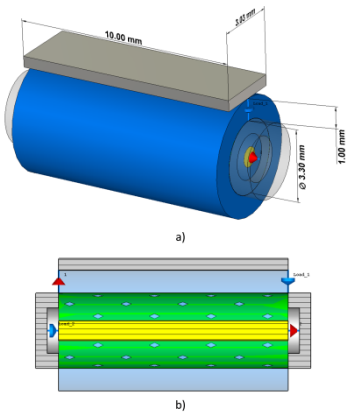

Fig. 1. a) Setup dimensions. b) Cross-sectional side view of line injection simulation model.

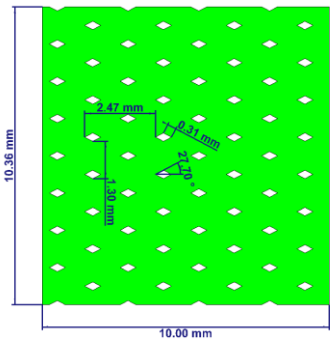

Fig. 2. Planar view of the shield used for simulation considering Vance's definition with C = 16; N = 7; α = 27.7°; P=0.4055 mm.

Fig. 3 shows the density of surface current in the model at 200 kHz, 2 MHz and 20 MHz. It is obvious that in this configuration the current distribution is not uniform in the cable shield under test. At 200 kHz the predominant effect is the diffusion, whereas at 20 MHz the coupling by small openings is more significant. As can be seen, at 3 MHz occurs the transition between these two dominant phenomena.

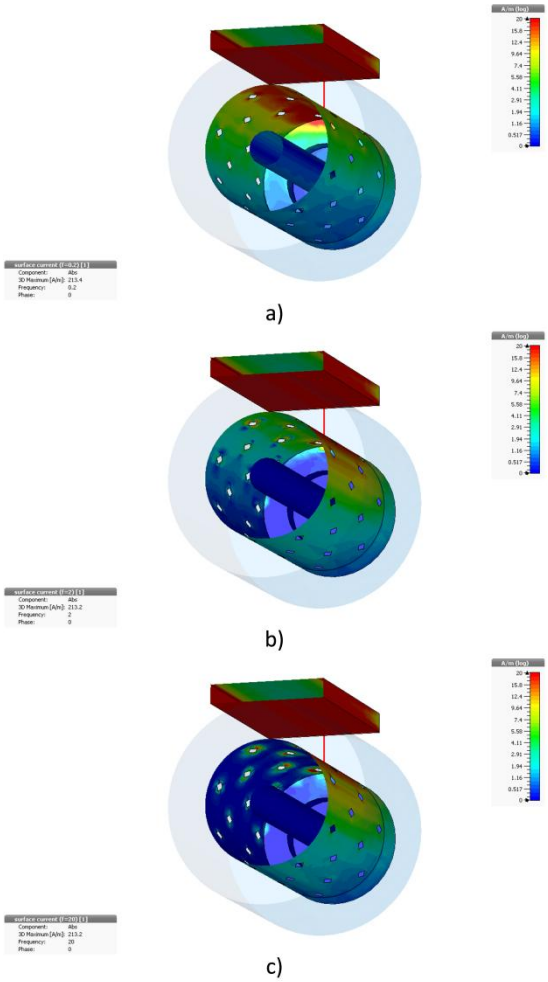

Fig. 3. Surface current density distribution in line injection simulation. a) 200 kHz. b) 2 MHz c) 20 MHz.

Transfer impedance obtained through the simulation of the line injection method presented a closer result to the Vance analytical model, as shown in Fig. 4. This was expected since the simplified model does not consider effects caused by carriers superposition and the depth of aperture through which eddy currents circulate. The difference in respect to Vance's model can be explained by the fact that their model considers the openings as ellipses, whereas in the simulated case apertures were modeled by diamonds, which is more similar to physical construction of shields. Further explorations increasing the size of the sample and also refining the mesh did not result in a better correlation.

B. Triaxial Method Simulation

As shown in Fig. 5, in this case the excitation signal is injected at the right end of the cable between the outer conductor and the cable shield, which is short-circuited to the wire core. At the opposite end only the shield is electrically connected to the return circuit, while the internal conductor is left open. In order to obtain a faster simulation the internal conductor was replaced by a voltage monitor. In addition, the outer cylinder to which the cable is concentrically positioned has its outer surfaces flat so as to perfectly fit the area considered in the simulation domain and a zero electric field (Et=0) boundary condition could be applied.

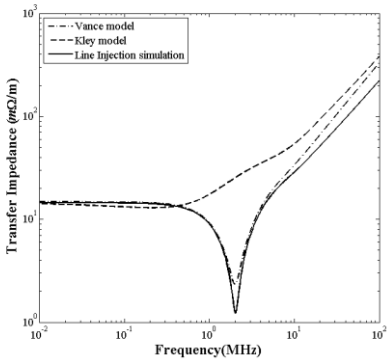

Fig. 4. Simulated line injection method compared to analytical models.

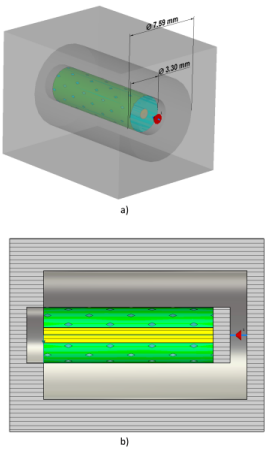

Fig. 5. a) dimensions of coaxial line formed by the tube and shield under test. b) simulation setup for triaxial method.

In this configuration the current density distribution in the shield is uniform (see Fig. 6), since the current return is distributed along the outer conductor. It is shown that at low frequency, the region in which the coupling is mainly due to diffusion effect, the current has almost the same intensity in all the surface of the shield. However, at 20 MHz a higher concentration near the openings is observed due to the predominance of this coupling mechanism in this frequency band.

As expected, since the cable model is the same and mesh is constructed in a similar way, the Z_t obtained with the triaxial method present good correlation with previously obtained with the line injection method (see Fig. 7), and both presented good agreement with Vance's model.

For shields with constructional characteristics close to those modeled by Vance and Kley, analytical calculation presents a good and fast estimate of Z_t value, however, in case of geometries not modeled by analytical models, 3D simulation of a simplified model is a good alternative to evaluate the most appropriate Z_t value to be used.

Simulations were performed on a Dell T5600 computer with two processors Intel Xeon 4-core E5-1620 V3 @ 3.5 GHz and 128 GB of RAM. Table 1 presents a comparison of the computational effort undertaken in the two simulations.

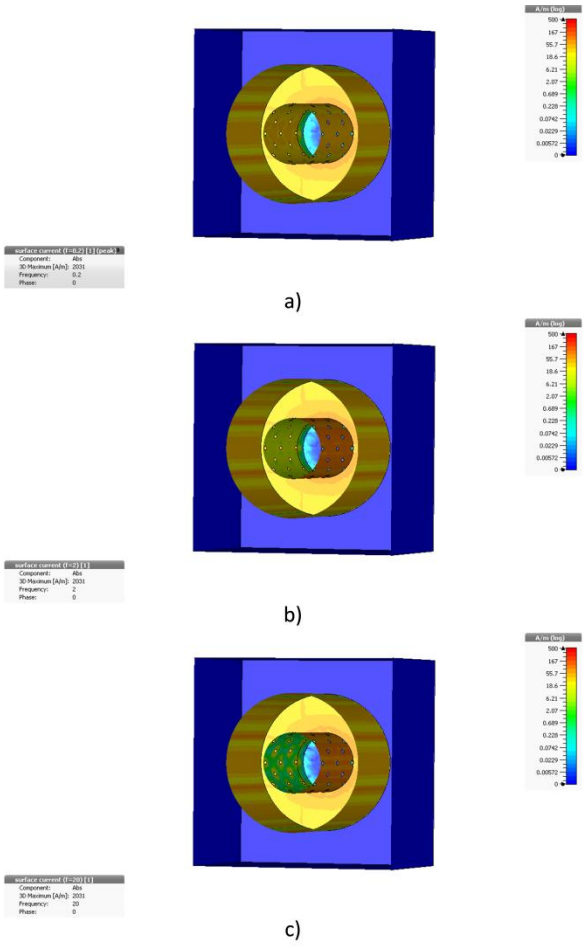

Fig. 6. Surface current density distribution in triaxial simulation. a) 200 kHz. b) 2 MHz c) 20 MHz.

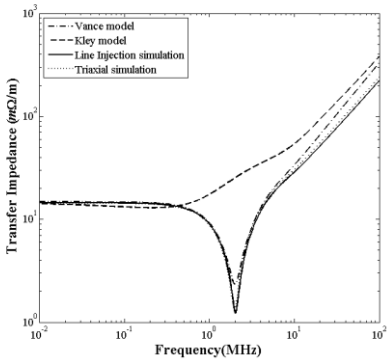

Fig. 7. Comparison between simulations of the measurement methods and analytical models.

TABLE I. COMPUTATIONAL EFFORT COMPARISON

Parameters	Line Injection	Triaxial
Number of cells	711.360	705.672
Memory allocated (Mbytes)	136.107	117.636
Simulation Time	4h 13 min	6h 35min

V. MEASUREMENTS

Although there is a construction procedure to provide a shield with the required parameters, the resultant shield is not always uniform. As can be seen in Fig. 8, in the same cable some carriers have different number of filaments. In addition, apertures have different sizes along the cable, probably due to the flexion and twist which the cable is subjected. Thus, it is interesting to measure the transfer impedance of these cables and compare to analytical models to evaluate how these possible manufacturing quality escapes influence on the shield transfer impedance. This should be considered as uncertainties in Z_t models used for CEM simulations. Cable parameters of Fig. 8, which were used as measurement species of 0.5m of length, are shown in Table 2.

Measurements were performed on a Rohde & Schwarz ZVL6 vector network analyzer whose measurement range is 9 kHz to 6 GHz. The equipment has been configured to provide a maximum output power of 20 dBm with 0dB attenuation at the ports. The measurement was performed through a logarithmic frequency scan with 4001 dots between 9 kHz and 100 MHz. The equipment was adjusted to provide the average result of 16 independent sequential scans.

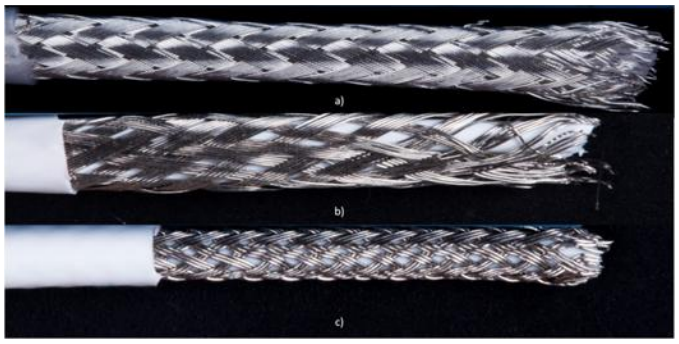

Fig. 8. Shield of measured cables. a) Coaxial cable. b) Twisted shield pair. c) Single shielded cable.

TABLE II. MEASURED SHIELDED CABLE PARAMETERS.

Parameters	Coaxial Cable	Twisted shielded pair	Single shielded
Shielding Diameter (mm)	3.2	2.9	1.6
Dielectric diameter (mm)	2.7	1.35	1.1
Diameter filament (AWG)	38	38	38
Number of carriers	16	16	12
Filaments per carrier	8	5/6	3
α	30o	25.2o	21.5o
Optical Coverage	96%	73%	69%

The line injection in this setup consists of an electrolytic copper foil covered with a polycarbonate insulation coating on one side with a self-adhesive material in which cables are centrally bonded to the tape.

The triaxial geometry was obtained using a cylindrical copper tube of 1.4 cm internal diameter. Case C of IEC 62153-4 -6, which replace the terminating resistor and the damping resistor to a short circuit, was used in order to reduce effect of capacitive coupling.

Measurements performed on coaxial cable are presented in Fig. 9. The line injection method, sampling the transient voltage at the far end extremity, showed the best correlation with Kley's model.

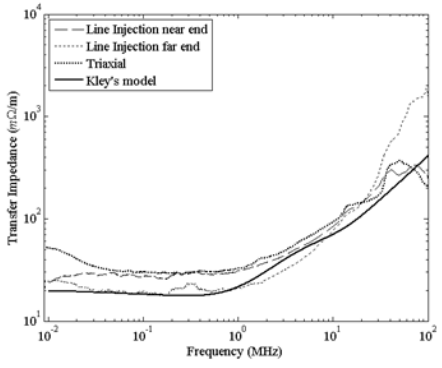

Fig. 9. Coaxial cable measurements.

Due to a smaller number of wires per carrier, the Z_t value of the twisted shielded pair was slightly higher (see in Fig. 10). Moreover, the non uniformity of the apertures results in a different current distribution in the shield due to the characteristics of two measurement methods, and caused a greater difference between the measured values for frequencies above 10 MHz in which coupling by small openings is the dominant phenomenon.

As shown in Fig. 11, the measured Z_t value for the single shielded cable is significantly higher in relation to others. This results from the lower number of carriers and wires per carrier in the shielding of this cable.

In addition, for this cable Vance and Kley models exhibit a major divergence in high frequency due to the smaller optical coverage of the shield and, the decrease of the ratio between the radius of the shield and its filament diameter, which is a criterion of validity of Vance's model (a>>d). Therefore, the models have their accuracy reduced.

It is important to note that the cut-off frequency of the measurement with the triaxial method is close to 50 MHz which is slightly below the expected 60 MHz value for a setup with 0.5 meters of coupling length, due to minor impedance mismatches on test setup.

As a consequence of the manufacturing process, variations of up to ± 8° in the weave angle are still in agreement with standard cable specifications. Fig. 12 shows the Z_t sensitivity regarding this parameter.

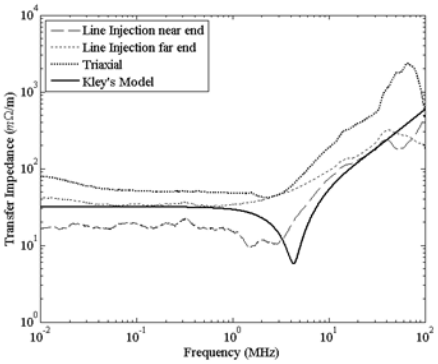

Fig. 10. Twisted shielded pair measurements.

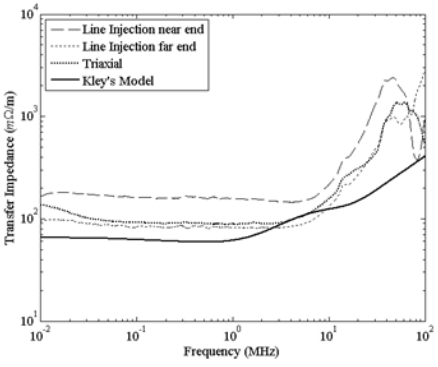

Fig. 11. Single shielded cable measurements.

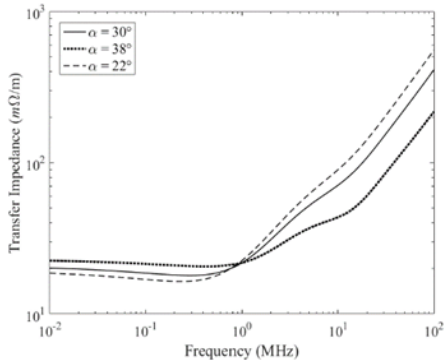

Fig. 12. Sensitivity analysis of α.

Number of filaments per carrier and shield filament diameter could also vary in a series production. The sensitivity analyses in relation to these parameters are presented in Fig. 13 and Fig. 14, respectively.

VI. Conclusions

Two experimental methods were used to characterize the surface transfer impedance of three different cable shields. A 3D simulation was performed to provide a better understanding of each setup characteristics and determine the dominant coupling mechanism for each frequency band. The combination of different techniques proved to be an interesting toolkit for evaluation of shielding properties especially for cable manufacturers.

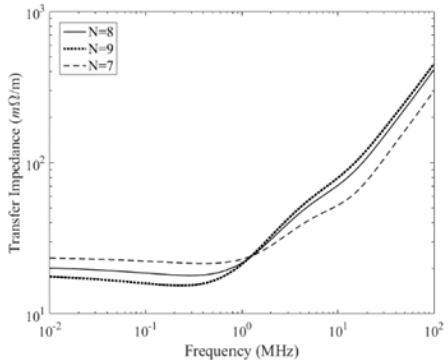

Fig. 13. Sensitivity analysis of filaments per carrier.

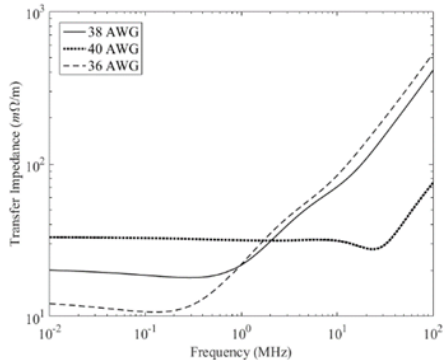

Fig. 14. Sensitivity analysis of filaments wire gauge.

For lower frequency lightning coupling, in which the energy content of coupled transients does not exceed 1MHz [13], the transfer impedance can be approximated by the dc resistance, whereas for multiple burst or HIRF conducted susceptibility analysis the inductive effect cannot be neglected.

A sensitivity analysis of Z_t, with respect to its weaving parameters, is useful to understand how the surface transfer impedance is affected by the tolerances related to manufacturing constraints and cables of different quality. Therefore, in the absence of empirical data with enough statistical sampling, it is recommended to incorporate margins based on the sensitivity analysis to account for the physical variations in the Z_t parameters.

References

[1] SAE ARP5415A, "User's manual for certification of aircraft electrical/electronic systems for indirect effects of lightning".

[2] I. G. Hansen and B. H. Kenney, "Specification and testing for power by wire aircraft," in 28th Intersociety Energy Conversion Engineering Conference, Atlanta, Georgia, August, 1993.

[3] J. L. Rotgerink, H. Schippers, J. Verpoorte and K. Nuyten, "EMC aspects of compact wiring for future aircraft," 2018 IEEE International Symposium on Electromagnetic Compatibility and 2018 IEEE Asia-Pacific Symposium on Electromagnetic Compatibility (EMC/APEMC), Singapore, 2018, pp. 165-170.

[4] R. Otin, J. Verpoorte and H. Schippers, "Finite element model for the computation of the transfer impedance of cable shields," in IEEE Transactions on Electromagnetic Compatibility, vol. 53, no. 4, pp. 950-958, Nov. 2011.

[5] E. F. Vance, "Shielding effectiveness of braided-wire shields," in IEEE Transactions on Electromagnetic Compatibility, vol. EMC-17, no. 2, pp. 71-77, May 1975.

[6] T. Kley, "Optimized single-braided cable shields," in IEEE Transactions on Electromagnetic Compatibility, vol. 35, no. 1, pp. 1-9, Feb. 1993.

[7] S. A. Schelkunoff, "The electromagnetic theory of coaxial transmission lines and cylindrical shields," in The Bell System Technical Journal, vol. 13, no. 4, pp. 532-579, Oct. 1934.

[8] INTERNATIONAL ELECTROTECHNICAL COMMISSION. IEC 62153-4-6: 2006: Metallic communication cable test methods - Part 4-6: Electromagnetic compatibility (EMC) - surface transfer impedance - line injection method. Geneva: [s.n.], 2006.

[9] INTERNATIONAL ELECTROTECHNICAL COMMISSION. IEC 62153-4-3: 2013:Metallic communication cable test methods - Part 4-3: Electromagnetic compatibility (EMC) — surface transfer impedance — triaxial method. Geneva: [s.n.], 2013.

[10] B. Démoulin and L. Koné, "Shielded cables transfer impedance measurement," in IEEE EMC Newsletter, n. 227, p. 38-45, 2010.

[11] YORK EMC SERVICES. How to use a CCC01 to measure cable shielding effectiveness through transfer impedance. Heslington. [2016?]. (Y8680FLY4).

[12] https://www.cst.com/products/cstmws/Solvers/TLM-Solver

[13] SAE ARP5412B, "Aircraft lightning environment and related test waveforms".